

Syntheses and Electronic Structures of One-Electron-Oxidized Group 10 Metal(II)–(Disalicylidene)diamine Complexes (Metal = Ni, Pd, Pt)

Yuichi Shimazaki,^{*,†} Tatsuo Yajima,[‡] Fumito Tani,[†] Satoru Karasawa,[§]
Koichi Fukui,^{¶,⊥} Yoshinori Naruta,[†] and Osamu Yamauchi^{*,‡}

Contribution from the Institute for Materials Chemistry and Engineering, Kyushu University, Higashi-ku, Fukuoka 812-8581, Japan, Unit of Chemistry, Faculty of Engineering, Kansai University, Suita, Osaka 564-8680, Japan, Graduate School of Pharmaceutical Sciences, Kyushu University, Higashi-ku, Fukuoka 812-8582, Japan, and Department of Chemistry, School of Science and Engineering, Waseda University, Shinjuku-ku, Tokyo 169-8555, Japan

Received September 30, 2006; E-mail: yshima@ms.ifoc.kyushu.ac.jp; osamuy@ipcku.kansai-u.ac.jp

Abstract: Group 10 metal(II) complexes of H₂tbu-salen (H₂tbu-salen = *N,N'*-bis(3',5'-di-*tert*-butylsalicylidene)ethylenediamine) and H₂tbu-salcn (H₂tbu-salcn = *N,N'*-bis(3',5'-di-*tert*-butylsalicylidene)-1,2-cyclohexanediamine) containing two 2,4-di(*tert*-butyl)phenol moieties, [Ni(tbu-salen)] (**1a**), [Ni(tbu-salcn)] (**1b**), [Pd(tbu-salen)] (**2a**), [Pd(tbu-salcn)] (**2b**), and [Pt(tbu-salen)] (**3**), were prepared and structurally characterized by X-ray diffraction, and the electronic structures of their one-electron-oxidized species were established by spectroscopic and electrochemical methods. All the complexes have a mononuclear structure with two phenolate oxygens coordinated in a very similar square-planar geometry. These complexes exhibited similar absorption spectra in CH₂Cl₂, indicating that they all have a similar structure in solution. Cyclic voltammograms of the complexes showed a quasi-reversible redox wave at $E_{1/2} = 0.82\text{--}1.05$ V (vs Ag/AgCl), corresponding to formation of the relatively stable one-electron-oxidized species. The electrochemically oxidized or Ce(IV)-oxidized species of **1a**, **2a**, and **3** displayed a first-order decay with a half-life of 83, 20, and 148 min at -20 °C, respectively. Ni(II) complexes **1a** and **1b** were converted to the phenoxyl radicals upon one-electron oxidation in CH₂Cl₂ above -80 °C and to the Ni(III)–phenolate species below -120 °C. The temperature-dependent conversion was reversible with the Ni(III)–phenolate ground state and was found to be a valence tautomerism governed by the solvent. One-electron-oxidized **1b** was isolated as [Ni(tbu-salcn)]NO₃ (**4**) having the Ni(II)–phenoxyl radical ground state. One-electron-oxidized species of the Pd(II) complexes **2a** and **2b** were different from those of the Ni(II) complexes, the Pd(II)–phenoxyl radical species being the ground state in CH₂Cl₂ in the range 5–300 K. The one-electron-oxidized form of **2b**, [Pd(tbu-salcn)]NO₃ (**5**), which was isolated as a dark green powder, was found to be a Pd(II)–phenoxyl radical complex. On the other hand, the ESR spectrum of the one-electron-oxidized species of Pt(II) complex **3** exhibited a temperature-independent large *g* anisotropy in CH₂Cl₂ below -80 °C, while its resonance Raman spectrum at -60 °C displayed ν_{Ba} of the phenoxyl radical band at 1600 cm⁻¹. These results indicated that the ground state of the Pt(II)–phenoxyl radical species has a large distribution of the radical electron spin at the Pt center. One-electron oxidation of **3** gave [Pt(tbu-salen)]NO₃ (**6**) as a solid, where the oxidation state of the Pt center was determined to be ca. +2.5 from the XPS and XANES measurements.

Introduction

The redox properties of metal complexes with potentially open-shell ligands are of current interest, and a number of studies have been devoted to obtaining an exact description of their oxidation states.^{1–3} Especially the coordination chemistry of the phenoxyl radical has been intensively studied in recent years

due to its occurrence in the active site of galactose oxidase, which contains one copper ion and oxidizes a primary alcohol to the aldehyde in the presence of dioxygen.^{2–11} The electronic

[†] Institute for Materials Chemistry and Engineering, Kyushu University.

[‡] Kansai University.

[§] Faculty of Pharmaceutical Sciences, Kyushu University.

[¶] Waseda University.

[⊥] Present address: Graduate School of Life Science and Systems Engineering, Kyushu Institute of Technology, Hibikino 2-4, Wakamatsuku, Kitakyushu 808-0196, Japan.

(1) Hendrickson, D. N.; Pierpont, C. G. In *Spin-Crossover in Transition Metal Compounds*; Gütllich, P., Goodwin, H. A., Eds.; Topics in Current Chemistry 234; Springer: Berlin, 2004; p 63.

(2) (a) Verani, C. N.; Gallert, S.; Bill, E.; Weyhermüller, T.; Wieghardt, K.; Chaudhuri, P. *Chem. Commun.* **1999**, 1747. (b) Chaudhuri, P.; Verani, C. N.; Bill, E.; Bothe, E.; Weyhermüller, T.; Wieghardt, K. *J. Am. Chem. Soc.* **2001**, *123*, 2213. (c) Chun, H.; Verani, C. N.; Chaudhuri, P.; Bothe, E.; Bill, E.; Weyhermüller, T.; Wieghardt, K. *Inorg. Chem.* **2001**, *40*, 4157. (d) Chun, H.; Weyhermüller, T.; Bill, E.; Wieghardt, K. *Angew. Chem., Int. Ed.* **2001**, *40*, 2489. (e) Herebian, D.; Bothe, E.; Bill, E.; Weyhermüller, T.; Wieghardt, K. *J. Am. Chem. Soc.* **2001**, *123*, 10012. (f) Chun, H.; Chaudhuri, P.; Weyhermüller, T.; Wieghardt, K. *Inorg. Chem.* **2002**, *41*, 790.

structures of one-electron-oxidized forms of various metal–phenolate complexes have been shown to be mainly dependent on the metal ions.^{1–3,12,13} One-electron-oxidized Fe(III)–phenolate complexes were found to be Fe(III)–phenoxy radical species,¹² while oxidation of V(III)–phenolate complexes gave only the V(IV) and V(V) complexes, where no oxidation of the phenolate moiety was observed.¹³ The properties of metal–radical complexes are different from those of high-valent metal complexes, whose apparent oxidation state is identical with that of the metal–radical species.^{1–3,12,13} Cu(II)–phenoxy radical species are known to undergo magnetic exchange interactions between Cu(II) and the phenoxy radical,^{3,9} the spin state being very similar to that of the d⁸ low-spin diamagnetic species of mononuclear Cu(III) complexes.¹⁴ However, in our recent investigations, the properties of a series of Cu(II)–phenoxy radical complexes with tripodal ligands revealed that they can be ESR active, showing the $S = 1$ ground state at 5 K, that is, a weak ferromagnetic interaction between Cu(II) and phenoxy radical.⁹ Oxidation of the high-spin d⁸ Ni(II) complexes of the same series of ligands yielded Ni(II)–phenoxy radical species, which showed the $S = 1/2$ ground state with antiferromagnetic coupling between the Ni(II) ion and phenoxy radical electrons.¹⁵

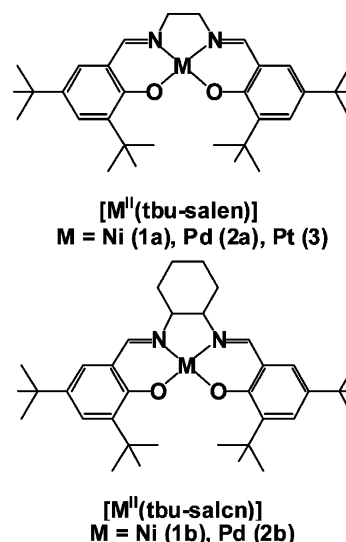


Figure 1. Structures of the complexes.

Most oxidized metal–phenolate complexes have been assigned to a single characteristic oxidation state, either a high-valent metal–phenolate or a metal–phenoxy radical state.

In contrast to these observations, we reported that oxidation of a low-spin d⁸ Ni(II)–salcn complex (salcn = *N,N'*-(disalicylidene)-1,2-cyclohexanediamine, deprotonated form) having salicylidene moieties with two bulky substituents leads to a temperature-dependent tautomerism between the Ni(II)–phenoxy radical and Ni(III)–phenolate states with the same $S = 1/2$ spin state in CH₂Cl₂ (Figure 1).¹⁶ Very recently, detailed studies on the oxidation locus of the one-electron-oxidized Ni(II)–salen-type complexes (salen = *N,N'*-(disalicylidene)ethylenediamine, deprotonated form) have been reported by Thomas et al.¹⁷ All these results suggested that the salen complexes of the other group 10 metal(II) ions Pd(II) and Pt(II), having the same electronic structure as the low-spin d⁸ Ni(II)–salen complexes, might show similar behavior upon one-electron oxidation.

In view of the fact that Pd(III) and Pt(III) complexes are rare as compared with Ni(III) complexes because of the open-shell d⁷ configuration,¹⁸ we have herein carried out comparative studies on synthesis of a series of the group 10 metal(II) complexes of salen-type ligands with bulky *tert*-butyl groups (Figure 1), chemical and electrochemical generation and isolation of the one-electron-oxidized species, and characterization of their electronic structures by various spectroscopic methods.

Experimental Section

Materials and Methods. All the chemicals used were of the highest grade available and were further purified whenever necessary.¹⁹ Solvents were also purified before use by standard methods.¹⁹ *N,N'*-Bis(3',5'-di-*tert*-butylsalicylidene)ethylenediamine (= H₂tbu-salen) and *N,N'*-bis(3',5'-di-*tert*-butylsalicylidene)-1,2-cyclohexanediamine (= H₂tbu-salcn)

- (3) (a) Müller, J.; Weyhermüller, T.; Bill, E.; Hildebrandt, P.; Ould–Moussa, L.; Glaser, T.; Wieghardt, K. *Angew. Chem., Int. Ed.* **1998**, *37*, 616. (b) Michel, F.; Torelli, S.; Thomas, F.; Duboc, C.; Philouze, C.; Belle, C.; Hamman, S.; Saint-Aman, E.; Pierre, J.-L. *Angew. Chem., Int. Ed.* **2005**, *44*, 438.
- (4) (a) Whittaker, M. M.; Whittaker, J. W.; Milburn, H.; Quick, A. J. *Biol. Chem.* **1990**, *265*, 9610. (b) McGlashen, M. L.; Eads, D. D.; Spiro, T. G.; Whittaker, J. W. *J. Phys. Chem.* **1995**, *99*, 4918. (c) Baron, A. J.; Stevens, C.; Wilmot, C.; Seneviratne, K. D.; Blakeley, V.; Dooley, D. M.; Phillips, S. E. V.; Knowles, P. F.; McPherson, M. J. *J. Biol. Chem.* **1994**, *269*, 25095. (d) Knowles, P. F.; Brown, R. D., III; Koenig, S. H.; Wang, S.; Scott, R. A.; McGuirl, M. A.; Brown, D. E.; Dooley, D. M. *Inorg. Chem.* **1995**, *34*, 3895. (e) Reynolds, M. P.; Baron, A. J.; Wilmot, C. M.; Vinecombe, E.; Steven, C.; Phillips, S. E. V.; Knowles, P. F.; MacPherson, M. J. *J. Biol. Inorg. Chem.* **1997**, *2*, 327.
- (5) Stubbe, J.; van der Donk, W. A. *Chem. Rev.* **1998**, *98*, 705.
- (6) Chaudhuri, P.; Wieghardt, K. *Prog. Inorg. Chem.* **2001**, *50*, 151.
- (7) Shimazaki, Y.; Huth, S.; Hirota, S.; Yamauchi, O. *Bull. Chem. Soc. Jpn.* **2000**, *73*, 1187.
- (8) (a) Shimazaki, Y.; Huth, S.; Odani, A.; Yamauchi, O. *Angew. Chem., Int. Ed.* **2000**, *39*, 1666. (b) Shimazaki, Y.; Huth, S.; Hirota, S.; Yamauchi, O. *Inorg. Chim. Acta* **2002**, *331*, 168.
- (9) (a) Halfen, J. A.; Young, V. G., Jr.; Tolman, W. B. *Angew. Chem., Int. Ed. Engl.* **1996**, *35*, 1687. (b) Halfen, J. A.; Jazdzewski, B. A.; Mahapatra, S.; Berreau, L. M.; Wilkinson, E. C.; Que, L., Jr.; Tolman, W. B. *J. Am. Chem. Soc.* **1997**, *119*, 8217. (c) Sokolowski, A.; Leutbecher, H.; Weyhermüller, T.; Schnepf, R.; Bothe, E.; Bill, E.; Hildebrandt, P.; Wieghardt, K. *J. Biol. Inorg. Chem.* **1997**, *2*, 444. (d) Zurita, D.; Gautier-Luneau, I.; Ménage, S.; Pierre, J.-L.; Saint-Aman, E. *J. Biol. Inorg. Chem.* **1997**, *2*, 46. (e) Jazdzewski, B. A.; Young, V. G., Jr.; Tolman, W. B. *Chem. Commun.* **1998**, 2521. (f) Benisvy, L.; Blake, A. J.; Collison, D.; Davis, E. S.; Garner, C. D.; McInnes, E. J. L.; McMaster, J.; Whittaker, G.; Wilson, C. *Chem. Commun.* **2001**, 1824. (g) Thomas, F.; Gellon, G.; Gautier-Luneau, I.; Saint-Aman, E.; Pierre, J.-L. *Angew. Chem., Int. Ed.* **2002**, *41*, 3047. (h) Philibert, A.; Thomas, F.; Philouze, C.; Hamman, S.; Saint-Aman, E.; Pierre, J.-L. *Chem. Eur. J.* **2003**, *9*, 3803.
- (10) Hockertz, J.; Steenken, S.; Wieghardt, K.; Hildebrandt, P. *J. Am. Chem. Soc.* **1993**, *115*, 11222.
- (11) Sokolowski, A.; Adam, B.; Weyhermüller, T.; Kikuchi, A.; Hildenbrand, K.; Schnepf, R.; Hildebrandt, P.; Bill, E.; Wieghardt, K. *Inorg. Chem.* **1997**, *36*, 3702.
- (12) (a) Whittaker, J. W. *Met. Ions Biol. Syst.* **1994**, *30*, 315. (b) Whittaker, J. W. In *Bioinorganic Chemistry of Copper*; Karlin, K. D., Tyeklar, Z., Eds.; Chapman & Hall: New York, 1993; p 447.
- (13) (a) Itoh, N.; Phillips, S. E. V.; Stevens, C.; Ogel, Z. B.; McPherson, M. J.; Keen, J. N.; Yadav, K. D. S.; Knowles, P. F. *Nature* **1991**, *350*, 87. (b) Itoh, N.; Phillips, S. E. V.; Stevens, C.; Ogel, Z. B.; McPherson, M. J.; Keen, J. N.; Yadav, K. D. S.; Knowles, P. F. *Faraday Discuss* **1992**, *93*, 75. (c) Itoh, N.; Phillips, S. E. V.; Yadav, K. D. S.; Knowles, P. F. *J. Biol. Chem.* **1994**, *238*, 794.
- (14) (a) Diaddario, L. L.; Robinson, W. R.; Margerum, D. W. *Inorg. Chem.* **1983**, *22*, 1021. (b) Hanss, J.; Krüger, H.-J. *Angew. Chem., Int. Ed. Engl.* **1996**, *35*, 2827. (c) Anson, F. C.; Collins, T. J.; Richmond, T. G.; Santarsiero, B. D.; Toth, J. E.; Treco, B. G. R. T. *J. Am. Chem. Soc.* **1987**, *109*, 2974. (d) Hanss, J.; Beckmann, A.; Krüger, H.-J. *Eur. J. Inorg. Chem.* **1999**, 163.
- (15) Shimazaki, Y.; Huth, S.; Karasawa, S.; Hirota, S.; Naruta, Y.; Yamauchi, O. *Inorg. Chem.* **2004**, *43*, 7816.

- (16) Shimazaki, Y.; Tani, F.; Fukui, K.; Naruta, Y.; Yamauchi, O. *J. Am. Chem. Soc.* **2003**, *125*, 10513.
- (17) (a) Rothaus, O.; Jarjaves, O.; Thomas, F.; Philouze, C.; Perez Del Vallee, C.; Saint-Aman, E.; Pierre, J.-L. *Chem. Eur. J.* **2006**, *12*, 2293. (b) Rothaus, O.; Thomas, F.; Jarjaves, O.; Philouze, C.; Saint-Aman, E.; Pierre, J.-L. *Chem. Eur. J.* **2006**, *12*, 6953.
- (18) Barnard, C. T. J.; Russel, M. J. H. In *Comprehensive Coordination Chemistry*; Wilkinson, G., Gillard, R. D., McCleverty, J. A., Eds.; Pergamon: Oxford, 1987; Vol. 5.
- (19) Perrin, D. D.; Armarego, W. L. F.; Perrin, D. R. *Purification of Laboratory Chemicals*; Pergamon Press: Elmsford, 1966.

(Figure 1) were prepared according to the literature.^{16,20,21} Electronic spectra were obtained with a Shimadzu UV-3101PC spectrophotometer. Electrochemical measurements were carried out in a conventional three-electrode cell for samples (1 mM) dissolved in dry CH₂Cl₂ or *N,N'*-dimethylformamide (DMF) containing 0.1 M tetra-*n*-butylammonium perchlorate (TBAP) with a BAS 100B electrochemical analyzer equipped with a glassy-carbon working electrode, a platinum wire used as a counter electrode, and a Ag/AgCl reference electrode. The reversibility of the electrochemical processes was evaluated by standard procedures and referenced against the ferrocene/ferrocenium redox couple. Electrospray ionization mass spectra (ESI-MS) were collected with a PE Sciex API 300 mass spectrometer. Frozen solution ESR spectra were acquired by a JEOL JES-RE1X X-band spectrometer equipped with a standard low-temperature apparatus. The spectra were recorded at 77 K by using quartz tubes with a 4-mm inner diameter. Microwave frequency was standardized against a Mn(II) marker. Resonance Raman spectra were obtained on a SpectraPro-300i spectrometer (Acton Research) with a 2400-groove grating, a Beamlok 2060 Kr ion laser (Spectra-Physics), a holographic supernoch filter (Kaiser Optical Systems), and an LN-1100PB CCD detector (Princeton Instruments) cooled with liquid N₂. Spectra were collected on solvated samples in spinning cells (2 cm diameter, 1500 rpm) at –60 °C at an excitation wavelength $\lambda_{\text{ex}} = 413.1$ nm (20 mW), 90° scattering geometry, and 5 min data accumulation. Peak frequencies were calibrated relative to indene and CCl₄ standards (accurate to ± 1 cm⁻¹). During each Raman experiment, UV/vis spectra were simultaneously collected on a PMA-11 CCD spectrophotometer (Hamamatsu) with a Photal MC-2530 (D₂/W₂) light source (Otsuka Electronic Co.). The X-ray photoelectron spectra (XPS) were recorded on a Thermo VG Scientific Model Theta Probe spectrometer using Al K α radiation (1486.6 eV), operated at 15 kV, 3 mA, as the X-ray excitation source. The solid sample was dispersed on an In film, and the carbon 1s binding energy (284.5 eV) was used to calibrate the binding energy.²² The X-ray absorption near-edge structures (XANES) were recorded on a Rigaku Looper X-ray absorption spectrometer with Si(400) double-crystal monochromator at room temperature. Mg K α radiation (1253.6 eV), operated at 10 kV, 20 mA, was used as the X-ray excitation source, and the energy resolution was estimated to be about 1.0 eV for Pt L_{III}-edge.

Syntheses of Complexes. **[Ni(tbu-salen)] (1a).** To a solution of H₂-tbu-salen²¹ (0.49 g, 1.0 mmol) in CH₂Cl₂ (10 mL) was added Ni(ClO₄)₂·6H₂O (0.37 g, 1.0 mmol) in CH₃OH (10 mL). A few drops of triethylamine was added to the resulting solution, which gave brown crystals upon standing at room temperature for 2–3 h. Elemental analysis (%) calcd for **1a** (C₃₂H₄₆N₂O₂Ni): C, 69.96; H, 8.44; N, 5.10. Found: C, 70.05; H, 8.41; N, 5.19. ¹H NMR (CDCl₃, 400 MHz): δ 7.47 (s, 2H), 7.28 (d, 2H), 6.85 (d, 2H), 3.28 (s, 4H), 1.39 (s, 18H), 1.24 (s, 18H).

[Ni(tbu-salcn)] (1b). Synthesis of this complex has been reported previously.¹⁶

[Pd(tbu-salen)] (2a). To a warm solution of H₂tbu-salen (0.49 g, 1.0 mmol) in C₂H₅OH (10 mL) was added Pd(CH₃COO)₂ (0.37 g, 1.0 mmol) in C₂H₅OH (10 mL). The resulting solution was boiled for a few minutes and kept standing at room temperature for 2–3 h to give a yellow precipitate. Recrystallization of the precipitate from CH₂Cl₂/MeOH gave yellow crystals. Elemental analysis (%) calcd for **2a** (C₃₂H₄₆N₂O₂Pd): C, 64.36; H, 7.76; N, 4.69. Found: C, 64.23; H, 7.71; N, 4.69. ¹H NMR (CDCl₃, 400 MHz): δ 7.76 (s, 2H), 7.42 (d, 2H), 6.97 (d, 2H), 3.72 (s, 4H), 1.47 (s, 18H), 1.26 (s, 18H).

[Pd(tbu-salcn)] (2b). This complex was prepared in a manner similar to that for **2a**. Elemental analysis (%) calcd for **2b** (C₃₆H₅₂N₂O₂Pd):

C, 66.40; H, 8.05; N, 4.30. Found: C, 66.53; H, 8.07; N, 4.28. ¹H NMR (CDCl₃, 400 MHz): δ 7.71 (s, 2H), 7.41 (d, 2H), 6.96 (d, 2H), 3.39 (m, 2H), 2.60 (m, 2H), 1.93 (m, 2H), 1.53 (s, 2H), 1.47 (s, 18H), 1.38 (m, 2H), 1.26 (s, 18H).

[Pt(tbu-salen)] (3). A mixture of Pt(en)Cl₂ (en = ethylenediamine) (0.50 g, 1.53 mmol), 3,5-di(*tert*-butyl)salicylaldehyde (0.72 g, 3.07 mmol), and triethylamine (0.31 g, 3.07 mmol) in absolute DMF (70 mL) was stirred for 10 days at 60 °C.²³ The reaction mixture was evaporated under a reduced pressure to give a brown solid, which was purified by silica gel column chromatography (CHCl₃/CH₃OH). Recrystallization from CH₂Cl₂/MeOH gave orange crystals. Elemental analysis (%) calcd for **3** (C₃₂H₄₆N₂O₂Pt): C, 56.04; H, 6.76; N, 4.08. Found: C, 56.11; H, 6.71; N, 4.09. ¹H NMR (CDCl₃, 400 MHz): δ 8.10 (s, 2H), 7.56 (d, 2H), 7.06 (d, 2H), 3.70 (s, 4H), 1.50 (s, 18H), 1.27 (s, 18H).

[Ni(tbu-salcn)]NO₃ (4). To a solution of [Ni(tbu-salcn)] (**1b**) (0.603 g, 1.0 mmol) in CH₂Cl₂ (15 mL) was added (NH₄)₂Ce(NO₃)₆ (0.548 g, 1.0 mmol) in CH₃CN (5 mL). A few drops of diethyl ether was added to the resulting solution, which was kept standing for 2–3 days at –80 °C to give a green powder. Elemental analysis (%) calcd for **4** (C₃₆H₅₂N₃O₅Ni): C, 64.97; H, 7.88; N, 6.31. Found: C, 65.15; H, 7.60; N, 6.39.

[Pd(tbu-salcn)]NO₃ (5) and [Pt(tbu-salen)]NO₃ (6). These complexes were prepared in a manner similar to that described for [Ni(tbu-salcn)]NO₃ (**4**). Elemental analysis (%) calcd for **5** (C₃₆H₅₂N₃O₅Pd): C, 60.62; H, 7.35; N, 5.89. Found: C, 60.65; H, 7.39; N, 5.69. Elemental analysis (%) calcd for **6** (C₃₂H₄₆N₃O₅Pt): C, 51.40; H, 6.20; N, 5.62. Found: C, 51.65; H, 6.19; N, 5.69.

X-ray Structure Determination. The X-ray experiments were carried out for the well-shaped single crystals of complexes **1a**, **2a**, and **3** on a Rigaku RAXIS imaging plate area detector with graphite-monochromated Mo K α radiation ($\lambda = 0.71073$ Å). The crystals were mounted on a glass fiber. In order to determine the cell constants and orientation matrix, three oscillation photographs were taken for each frame, with the oscillation angle of 3° and the exposure time of 3 min. Reflection data were corrected for both Lorentz and polarization effects. The structures were solved by the heavy-atom method and refined anisotropically for non-hydrogen atoms by full-matrix least-squares calculations. Each refinement was continued until all shifts were smaller than one-third of the standard deviations of the parameters involved. Atomic scattering factors and anomalous dispersion terms were taken from the literature.²⁴ Hydrogen atoms, except for those of the water molecules, were located at the calculated positions and were assigned a fixed displacement and constrained to ideal geometry with C–H = 0.95 Å. The thermal parameters of calculated hydrogen atoms were related to those of their parent atoms by $U(\text{H}) = 1.2U_{\text{eq}}(\text{C})$. All the calculations were performed by using the TEXSAN program package.²⁵ Summaries of the fundamental crystal data and experimental parameters for structure determination are given in Table S1.

Results and Discussion

Preparation and General Characterization of [M(tbu-salen)] Complexes (M = Ni, Pd, and Pt). N₂O₂-donor chelating ligands, H₂tbu-salen and H₂tbu-salcn²¹ (Figure 1), reacted with Ni(ClO₄)₂·6H₂O and triethylamine in CH₃OH/CH₂Cl₂ to give [Ni(tbu-salen)] (**1a**) and [Ni(tbu-salcn)] (**1b**), respectively, as brownish-yellow crystals. [Pd(tbu-salen)] (**2a**) and [Pd(tbu-salcn)] (**2b**) were synthesized by the reaction of Pd(CH₃COO)₂ with the respective ligands in a similar manner as yellow

(20) For example, see: Calligar, M.; Randacci, L.; Nardin, G. *Coord. Chem. Rev.* **1972**, *7*, 385.

(21) Jacobsen, E. N.; Zhang, W.; Muci, A. R.; Ecker, J. R.; Deng, L. *J. Am. Chem. Soc.* **1991**, *113*, 7063.

(22) Chastain, J.; King, R. G., Jr. *Handbook of X-ray Photoelectron Spectroscopy*; Physical Electronics, Inc.: Chanhassen, MN, 1995.

(23) Hall, D.; Sheat, S. V.; Waters, T. N. *J. Chem. Soc. A* **1968**, 460.

(24) Ibers, J. A.; Hamilton, W. C. *International Tables for X-Ray Crystallography*; Kynoch: Birmingham, 1974; Vol. IV.

(25) *Crystal Structure Analysis Package*; Molecular Structure Corp.: The Woodlands, TX, 1985 and 1999.

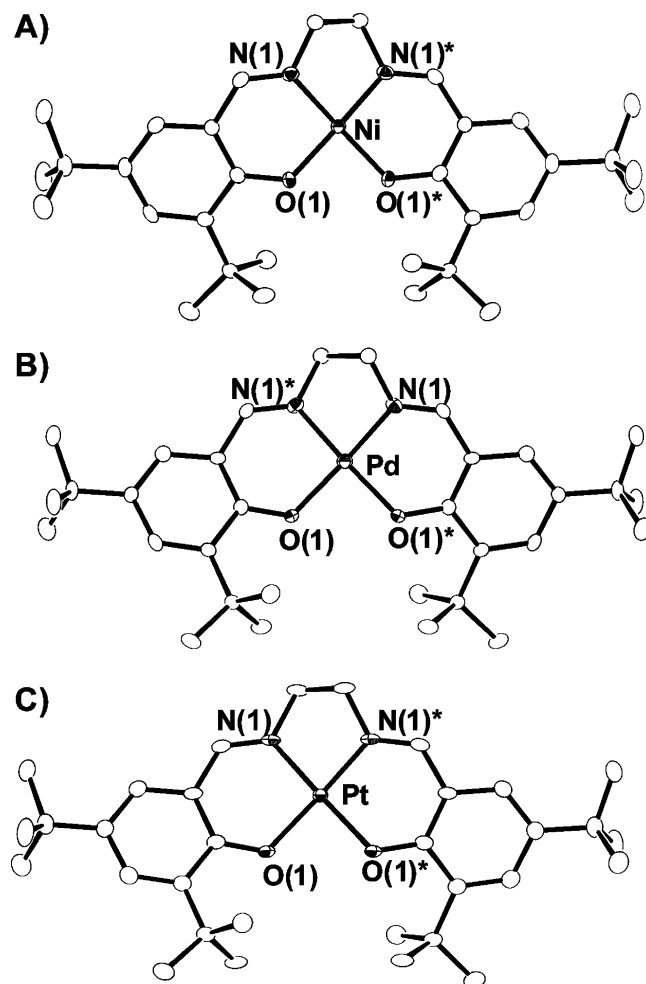


Figure 2. ORTEP views of $[M^{\text{II}}(\text{tbu-salen})]$, drawn with the thermal ellipsoids at the 50% probability level and atomic labeling scheme: (A) $[\text{Ni}^{\text{II}}(\text{tbu-salen})]$ (**1a**), (B) $[\text{Pd}^{\text{II}}(\text{tbu-salen})]$ (**2a**), and (C) $[\text{Pt}^{\text{II}}(\text{tbu-salen})]$ (**3**).

crystals. $[\text{Pt}(\text{tbu-salen})]$ (**3**) was prepared from $\text{Pt}(\text{en})\text{Cl}_2$ and 3,5-di(*tert*-butyl)salicylaldehyde as orange crystals.²³ The ORTEP views of *tbu-salen* complexes **1a**, **2a**, and **3** are shown in Figure 2, and selected bond lengths and angles are listed in Table 1. All the complexes have a square-planar C_{2v} geometry formed by two phenolato oxygen atoms and two imino nitrogen atoms.^{26–28} The M–N and M–O bond lengths (Ni–N = 1.846(2), Pd–N = 1.948(4), Pt–N = 1.950(3) Å; Ni–O = 1.846(2), Pd–O = 1.975(3), Pt–O = 1.995(2) Å) (Table 1) correspond well with those reported for nonsubstituted *salen* complexes.^{26,27} They increased in the order **1a** < **2a** < **3** (Table 1), which is in agreement with the order of the periodic table.^{26,27} The solutions of the complexes in CH_2Cl_2 showed a similar yellow color with characteristic absorption peaks at 300–600 nm (λ_{max} ($\epsilon/\text{M}^{-1}\text{cm}^{-1}$): **1a**, 346 (7800), 417 (6400), 440 (sh,

Table 1. Selected Bond Distances (Å) and Angles (deg) of Complexes **1a**, **2a**, and **3**

	1a (Ni)	2a (Pd)	3 (Pt)
Distances			
M(1)–O(1)	1.846(2)	1.975(3)	1.995(2)
M(1)–N(1)	1.846(2)	1.948(4)	1.950(3)
Angles			
O(1)–Ni(1)–O(1)*	86.3(1)	89.0(2)	87.2(1)
O(1)–Ni(1)–N(1)	94.36(9)	93.4(1)	94.4(1)
O(1)–Ni(1)–N(1)*	172.2(1)	174.7(1)	175.61(9)
O(1)*–Ni(1)–N(1)	172.2(1)	174.7(1)	175.61(9)
O(1)*–Ni(1)–N(1)*	94.36(9)	93.4(1)	94.4(1)
N(1)–Ni(1)–N(2)	86.1(2)	84.6(2)	84.4(2)

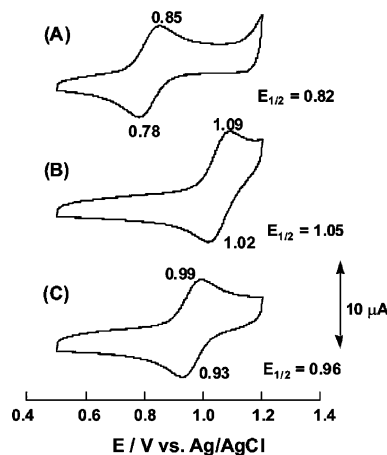


Figure 3. Cyclic voltammograms of $[\text{M}^{\text{II}}(\text{tbu-salen})]$ in CH_2Cl_2 (1.0 mM) containing 0.1 M *n*- Bu_4NClO_4 : (A) $[\text{Ni}^{\text{II}}(\text{tbu-salen})]$ (**1a**), (B) $[\text{Pd}^{\text{II}}(\text{tbu-salen})]$ (**2a**), and (C) $[\text{Pt}^{\text{II}}(\text{tbu-salen})]$ (**3**). Working electrode, glassy carbon; counter electrode, Pt wire; reference electrode, Ag/AgCl; scan rate, 100 mV s^{-1} .

4600), 550 nm (sh, 670); **2a**, 330 (sh, 5500), 411 (4900), 428 nm (5200); **3**, 315 (7700), 351 (9200), 432 (3300), 456 nm (3000). All the complexes, **1a,b**, **2a,b**, and **3**, were diamagnetic d^8 low-spin metal(II) species, since sharp ^1H NMR signals were observed in the diamagnetic region in CDCl_3 . The aromatic proton signals of the two phenol moieties in **1a**, **2a**, and **3** could not be distinguished from each other, and the signals for the ethylene protons were observed as a singlet, which indicates that the C_{2v} symmetry was maintained in solution. The chemical shifts of the phenol aromatic protons increased in the order **1a** < **2a** < **3**, indicating that the electron density on the phenol moiety decreases with the increasing atomic number of the metal ion (Figure S1). The cyclic voltammograms (CVs) of **1a**, **2a**, and **3**, recorded in CH_2Cl_2 under anaerobic conditions in the range 0.5–1.2 V vs Ag/AgCl (Figure 3), showed one quasi-reversible redox wave corresponding to the transfer of one electron at 0.82 V ($\Delta E = 0.07$ V) for **1a**, and similar redox waves were also observed for **2a** and **3** at 1.05 ($\Delta E = 0.07$ V) and 0.96 V ($\Delta E = 0.06$ V), respectively.¹⁶ The order of the redox potential was **1a** (Ni) < **3** (Pt) < **2a** (Pd), which shows that there is no correlation with the order of the metal–O bond lengths or the NMR chemical shifts of the phenol protons. An additional redox wave was observed for **1a** (1.22 V) and an irreversible oxidation peak for **3** (1.41 V), but no clear peak was detected for **2a**. On the other hand, $[\text{Ni}(\text{salen})]$, $[\text{Pd}(\text{salen})]$, and $[\text{Pt}(\text{salen})]$, all without bulky substituents, were found to give only an irreversible oxidation peak (E_{pa}) at 0.89, 1.12, and

(26) Castro, B.; Freire, C.; Duarte, M. T.; Piedade, M. F. M.; Santos, I. C. *Acta Crystallogr. Sect. C* **2001**, *57*, 370.

(27) Sawodny, W.; Thewalt, U.; Potthoff, E.; Ohl, R. *Acta Crystallogr. Sect. C* **1999**, *55*, 2060.

(28) (a) Freire, C.; Castro, B. *J. Chem. Soc., Dalton Trans.* **1998**, 1491. (b) Santos, I. C.; Vilas-Boas, M.; Piedade, M. F. M.; Freire, C.; Duarte, M. T.; Castro, B. *Polyhedron* **2000**, *19*, 655. (c) Castro, B.; Freire, C. *Inorg. Chem.* **1990**, *29*, 5113. (d) Carrondo, M. A. A. F. de C. T.; Castro, B.; Coelho, A. M.; Domingues, D.; Freire, C.; Morais, J. *Inorg. Chim. Acta* **1993**, *205*, 157. (e) Azevedo, F.; Carrondo, M. A. A. F. de C. T.; Castro, B.; Convery, M.; Domingues, D.; Freire, C.; Duarte, M. T.; Nielsen, K.; Santos, I. C. *Inorg. Chim. Acta* **1994**, *219*, 43.

0.93 V, respectively, in the range 0–1.2 V, in CH_2Cl_2 under the present conditions. These results indicate that **1a**, **2a**, and **3** could form one-electron-oxidized species which may be relatively stable. Electrochemical oxidation of **1a**, **2a**, and **3** at 1.2 V in CH_2Cl_2 revealed a transfer of more than 0.9 electron per molecule, with a concomitant color change from yellow to green at -60°C .¹⁶ The ESI mass spectra of the oxidized species of **1a**, **2a**, and **3** exhibited peaks at $m/z = 548$, 596, and 685, respectively, and the isotope pattern of each complex was in good agreement with the calculated one. Therefore, the one-electron-oxidized complexes are monocationic species, $[\text{M}(\text{tbusalen})]^+$ ($\text{M} = \text{Ni}, \text{Pd}, \text{Pt}$), which can be either $\text{M}(\text{III})$ –tbusalen or $\text{M}(\text{II})$ –phenoxy radical complexes.

Characterization of One-Electron-Oxidized Species in Solution. (a) Ni(II) Complexes 1a and 1b. Addition of an equimolar amount of $(\text{NH}_4)_2\text{Ce}(\text{NO}_3)_6$ to **1a** and **1b** in CH_2Cl_2 at low-temperature caused a color change from yellow to green. The absorption spectrum of oxidized **1a** exhibited characteristic new peaks at λ ($\epsilon/\text{M}^{-1}\text{cm}^{-1}$) = 311 (9100), 374 (7200), 430 (3500), 881 (1000), and 1103 nm (3000). Both electrochemical oxidation and chemical oxidation by $\text{Ce}(\text{IV})$ gave the same oxidized species. However, $\text{Ce}(\text{IV})$ oxidation in DMF was different; the absorption spectrum of oxidized **1a** in DMF exhibited peaks at λ ($\epsilon/\text{M}^{-1}\text{cm}^{-1}$) = 332 (11800), 414 (5900), 464 (5600), 630 (420), and 1134 nm (390), which corresponded well with those of the reported $\text{Ni}(\text{III})$ –Schiff base complexes.²⁷ The oxidized Ni complexes were relatively stable at -20°C , and plots of the absorbance vs time indicated that the intensity decrease was in a first-order manner. The half-life of oxidized **1a** in CH_2Cl_2 was 82.5 min ($k_{\text{obs}} = 1.40 \times 10^{-4}\text{ s}^{-1}$) at -20°C and 6.8 min ($k_{\text{obs}} = 1.70 \times 10^{-3}\text{ s}^{-1}$) at 20°C , and in DMF it was 6.5 min ($k_{\text{obs}} = 1.77 \times 10^{-3}\text{ s}^{-1}$) at 20°C , indicating that the stability of one-electron-oxidized **1a** is independent of the solvent and that it is less stable than the one-electron-oxidized Ni complexes of 3NIO-donor tripodal ligands containing a phenolate moiety.¹⁵ The properties of **1a** are in good agreement with those reported recently.^{17b}

We reported previously that the ESR spectrum of one-electron-oxidized **1a** in CH_2Cl_2 at temperatures below -120°C (Figure 4 B) exhibited parameters with a large g tensor anisotropy ($g_1 = 2.30$, $g_2 = 2.23$, $g_3 = 2.02$, and $g_{\text{av}} = 2.18$), indicating a rhombic symmetry typically known for the nickel-centered oxidized species.¹⁶ The spectrum corresponds with the spectra reported for the oxidized forms of $[\text{Ni}(\text{salen})]$ and $[\text{Ni}(\text{salcn})]$ and other $\text{Ni}(\text{III})$ –Schiff base complexes.²⁸ These observations are consistent with the formation of a six-coordinate $\text{Ni}(\text{III})$ complex, and oxidized **1a** at $< -120^\circ\text{C}$ can thus be formulated as a $\text{Ni}(\text{III})$ –phenolate complex with the metal center in a low-spin $^2\text{A}_1$ ground state.²⁹ In contrast to this, an isotropic signal appeared at $g_{\text{iso}} = 2.04$ (Figure 4A) with the decrease of the rhombic ESR signals in the temperature range -115 to -100°C . The integrated spectrum showed that the number of spins remains essentially the same in this temperature range, the amount of the unpaired electron being more than 0.85. Since the intense $g_{\text{iso}} = 2.04$ signal is different from the g_{av} value obtained from other $\text{Ni}(\text{III})$ –Schiff base complexes,²⁸ it was concluded to be the isotropic signal of a $\text{Ni}(\text{II})$ –phenoxy radical complex, in analogy with the other reported $\text{Ni}(\text{II})$ –ligand

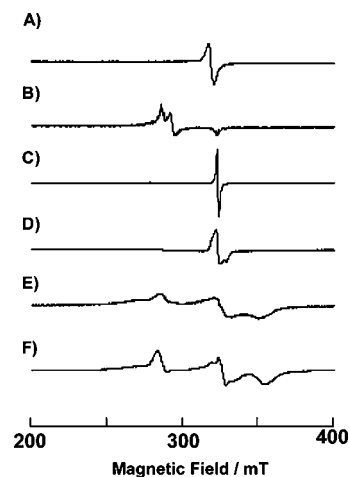


Figure 4. Temperature dependence of the ESR spectra of one-electron-oxidized **1a**, **2a**, and **3** in CH_2Cl_2 ($5.0 \times 10^{-4}\text{ M}$). Microwave power, 1 mW; modulation amplitude, 0.63 mT. (A) One-electron-oxidized **1a** at -60°C .¹⁶ (B) One-electron-oxidized **1a** at -140°C .¹⁶ (C) One-electron-oxidized **2a** at -60°C . (D) One-electron-oxidized **2a** at -140°C . (E) One-electron-oxidized **3** at -60°C . (F) One-electron-oxidized **3** at -140°C .

radical complexes.³⁰ The exchange between the oxidation states of the nickel ion was dependent on the temperature and reversible for the first few cycles. The same observations were also made for one-electron-oxidized **1b**. The transition temperature for interconversion of the metal- and ligand-centered oxidation states was found to depend on the solvent: in CHCl_3 (mp -63.5°C), the transition temperature is in the range -60 to -80°C , which is higher than that in CH_2Cl_2 (mp -95°C) (Figure S2). Similar results were reported by Thomas et al. for the one-electron-oxidized $\text{Ni}(\text{II})$ complexes of salen-type ligands.¹⁷ This suggests that a phase transition in the solvent may be responsible for the interconversion.^{17a}

On the other hand, our previous study showed that in DMF one-electron-oxidized **1a** exhibited the ESR signals characteristic of an axially symmetrical $S = 1/2$ $\text{Ni}(\text{III})$ –Schiff base complex ($g_1 = 2.27$, $g_2 = 2.22$, $g_3 = 2.02$, and $g_{\text{av}} = 2.17$) at $< -80^\circ\text{C}$ and an isotropic signal at $g_{\text{iso}} = 2.18$ at room temperature.¹⁶ By comparing the g_{iso} value with the g_{av} values of the $\text{Ni}(\text{III})$ complexes,^{16,17,28} we concluded that the one-electron-oxidized species in DMF is a six-coordinate $\text{Ni}(\text{III})$ –phenolate complex irrespective of the temperature.¹⁶

The resonance Raman spectra of **1b** and oxidized **1b** in the range 1400 – 1700 cm^{-1} , obtained in CH_2Cl_2 at -45°C , exhibited two intense bands at 1504 and 1605 cm^{-1} ,¹⁶ which are assigned to the characteristic ν_{7a} and ν_{8a} vibrational modes of phenoxy radicals predominantly including the C–O stretching and the C_{ortho} – C_{meta} stretching vibrations, respectively.^{31–35} This spectral feature is in good agreement with that of the Ni –

(29) Takvoryan, N.; Farmery, K.; Katovic, V.; Lovecchio, F. V.; Gore, E. S.; Anderson, L. B.; Cusch, D. H. *J. Am. Chem. Soc.* **1974**, *96*, 731.

(30) (a) Dolphin, D.; Niem, T.; Felton, R. H.; Fujita, I. *J. Am. Chem. Soc.* **1975**, *97*, 5288. (b) Chang, D.; Malinski, T.; Ulman, A.; Kadish, K. M. *Inorg. Chem.* **1984**, *23*, 817. (c) Dongho, K.; Miller, L. A.; Spiro, T. G. *Inorg. Chem.* **1986**, *25*, 2468. (d) Connick, P. A.; Macor, K. A. *Inorg. Chem.* **1991**, *30*, 4654. (e) Seth, J.; Palaniappan, V.; Bocian, D. F. *Inorg. Chem.* **1995**, *34*, 2201. (31) Müller, J.; Kikuchi, A.; Bill, E.; Weyhermüller, T.; Hildebrandt, P.; Ould-Moussa, L.; Wieghardt, K. *Inorg. Chim. Acta* **2000**, *297*, 265. (32) (a) Sokolowski, A.; Leutbecher, H.; Weyhermüller, T.; Schnepf, R.; Bothe, E.; Bill, E.; Hildebrandt, P.; Wieghardt, K. *J. Biol. Inorg. Chem.* **1997**, *2*, 444. (b) Sokolowski, A.; Müller, J.; Weyhermüller, T.; Schnepf, R.; Bill, E.; Hildebrandt, P.; Hildenbrand, K.; Bothe, E.; Wieghardt, K. *J. Am. Chem. Soc.* **1997**, *119*, 8889. (33) McGlashen, M. L.; Eads, D. D.; Spiro, T. G.; Whittaker, J. W. *J. Phys. Chem.* **1995**, *99*, 4918.

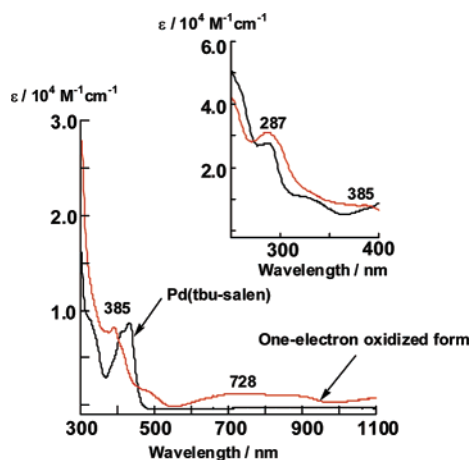


Figure 5. Absorption spectral change of **2a** before and after one-electron oxidation by 1 equiv of Ce(IV) at $-40\text{ }^{\circ}\text{C}$ in CH_2Cl_2 ($5.0 \times 10^{-4}\text{ M}$): black line, **2a**; red line, oxidized **2a**.

(II)–phenoxy radical complex using as ligand a 1,4,7-triaza-cyclononane derivative with a pendent phenol moiety.^{31,32} In contrast to this, the Raman spectrum of oxidized **1b** in DMF did not give the bands due to the phenoxy radical, in agreement with the finding that no phenoxy radical was formed in DMF. The solvent dependence of the oxidation state may be ascribed to the coordinating ability of the solvent, because DMF may have a higher affinity for the nickel center than CH_2Cl_2 ¹⁷ and thus stabilize the higher oxidation state.

(b) Pd(II) Complexes 2a and 2b. Oxidation of [Pd(tbu-salen)] (**2a**) by an equimolar amount of $(\text{NH}_4)_2\text{Ce}(\text{NO}_3)_6$ in CH_2Cl_2 at $-60\text{ }^{\circ}\text{C}$ caused a color change from yellow to green. Oxidation of [Pd(salen)] in CH_2Cl_2 at $-80\text{ }^{\circ}\text{C}$ caused decomposition reactions immediately, so that no intermediates were detected. One-electron-oxidized **2a** exhibited some new intense absorption peaks around 385 nm ($\epsilon = 8700$) and a broad band centered at 728 nm ($\epsilon = 1000$) (Figure 5). The difference between the one-electron-oxidized **1a** and **2a** is that the intense band around 1100 nm observed for **1a** was absent in **2a**. Further, one-electron-oxidized **2a** was the most unstable in CH_2Cl_2 in the group 10 metal–tbu-salen series, the half-life in CH_2Cl_2 being 20.2 min ($k_{\text{obs}} = 5.72 \times 10^{-4}\text{ s}^{-1}$) at $-20\text{ }^{\circ}\text{C}$ and 1.2 min ($k_{\text{obs}} = 9.59 \times 10^{-3}\text{ s}^{-1}$) at $20\text{ }^{\circ}\text{C}$, respectively. The ESR spectrum of oxidized **2a** above $-80\text{ }^{\circ}\text{C}$ showed a sharp isotropic signal at $g = 2.010$, while the spectrum below $-100\text{ }^{\circ}\text{C}$ displayed a rhombic signal at $g = 2.012$ with significant g anisotropy (Figure 4C,D). Similar observations were also made for one-electron-oxidized **2b**. These results indicate that the ground state of one-electron-oxidized **2a** and **2b** is Pd(II)–phenoxy radical species mixed with a small Pd ion character.³⁶

Further evidence for the Pd(II)–phenoxy radical bonding has been provided by comparison of the resonance Raman spectra for a Pd(II)–phenolate complex and its one-electron-oxidized species in the corresponding temperature range. The spectra of **2a** in the range $1100\text{--}1700\text{ cm}^{-1}$, obtained before and after Ce(IV) oxidation, disclosed that the bands observed

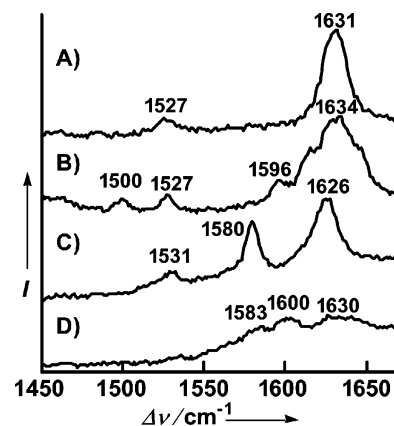


Figure 6. Resonance Raman spectra of Pd and Pt complexes, **2a** and **3**, and their one-electron-oxidized species (2.0 mM) at $-60\text{ }^{\circ}\text{C}$ in CH_2Cl_2 ($\lambda_{\text{ex}} = 413.1\text{ nm}$, 20 mW): (A) **2a**. (B) one-electron-oxidized **2a**. (C) **3**, and (D) one-electron-oxidized **3**.

for **2a** disappeared upon oxidation to give intense bands at 1500 and 1596 cm^{-1} (Figure 6A,B), which are assigned to the ν_{7a} and ν_{8a} vibrational modes of phenoxy radicals, respectively.^{31–35} As described in the previous section, the positions of the bands as well as their Raman intensity ratio can be used for distinguishing between coordinated and uncoordinated phenoxy radicals.^{31,32} The frequency difference, $\nu_{8a} - \nu_{7a}$, and the Raman intensity ratio, $I(\nu_{8a})/I(\nu_{7a})$, have been reported to be $>90\text{ cm}^{-1}$ and >1 , respectively, for metal-coordinated phenoxy radicals and $<90\text{ cm}^{-1}$ and <0.1 , respectively, for uncoordinated radicals.^{31,32} Oxidized **2a** at $-60\text{ }^{\circ}\text{C}$ exhibited $\nu_{8a} - \nu_{7a} = 96\text{ cm}^{-1}$ and $I(\nu_{8a})/I(\nu_{7a}) \approx 1$ (Figure 6B), which are close to the values for a coordinated phenoxy radical species. Thus, the ground state of one-electron-oxidized **2a** is concluded to be mainly the Pd(II)–phenoxy radical state mixed with a small Pd ion character, as reported for one-electron-reduced bis(*o*-iminobenzosemiquinonato)palladium(II) complexes.³⁶ In this connection, the 1527 cm^{-1} Raman band was observed before and after oxidation of **2a** and may be assigned to the ν_{19a} vibration of the phenolate moieties,³³ while the corresponding band for the Ni and Pt complexes in CH_2Cl_2 disappeared after one-electron oxidation. Considering that the band was observed for the Ni(III)–phenolate complex in DMF,¹⁶ these observations may indicate that the radical electron is localized on one of the two phenolate moieties in **2a** at $-60\text{ }^{\circ}\text{C}$. This is in contrast with the one-electron-oxidized Ni(II)–salen complex, where the Ni(II) center has a nonnegligible Ni(III) character¹⁶ and the singly occupied molecular orbital (SOMO) of the ligand is equally developed on both phenoxy moieties, indicating the delocalization of the unpaired electron.^{17a}

(c) Pt(II) Complex 3. One-electron oxidation of [Pt(tbu-salen)] (**3**) in CH_2Cl_2 at $-60\text{ }^{\circ}\text{C}$ caused a color change to green. The absorption spectrum of oxidized **3** showed new intense bands at λ ($\epsilon/\text{M}^{-1}\text{ cm}^{-1}$) = 300 (30000), 360 (sh, 10000), 452 (2300), 491 (2100), 628 (1200), 716 (1100), 850 (sh, 3200), and 972 nm (9400) (Figure 7). Though these absorption bands were also observed in DMF, the stability of oxidized **3** in DMF was lower than that in CH_2Cl_2 , and the half-life of oxidized **3** was 148 min ($k_{\text{obs}} = 7.79 \times 10^{-5}\text{ s}^{-1}$) at $-20\text{ }^{\circ}\text{C}$ and 8.8 min ($k_{\text{obs}} = 1.31 \times 10^{-3}\text{ s}^{-1}$) at $20\text{ }^{\circ}\text{C}$ in CH_2Cl_2 and 4.0 min ($k_{\text{obs}} = 2.90 \times 10^{-3}\text{ s}^{-1}$) at $20\text{ }^{\circ}\text{C}$ in DMF. Comparison of the half-life values measured in CH_2Cl_2 revealed that oxidized **3** is the

(34) Babcock, G. T.; El-Deeb, M. K.; Sandusky, P. O.; Whittaker, M. M.; Whittaker, J. W. *J. Am. Chem. Soc.* **1992**, *114*, 3727.

(35) (a) Tripathi, G. N. R.; Schuler, R. H. *J. Phys. Chem.* **1988**, *92*, 5129. (b) Johnson, C. R.; Ludwig, M.; Asher, S. A. *J. Am. Chem. Soc.* **1986**, *108*, 905.

(36) Min, K. S.; Weyhermüller, T.; Bothe, E.; Wieghardt, K. *Inorg. Chem.* **2004**, *43*, 2922.

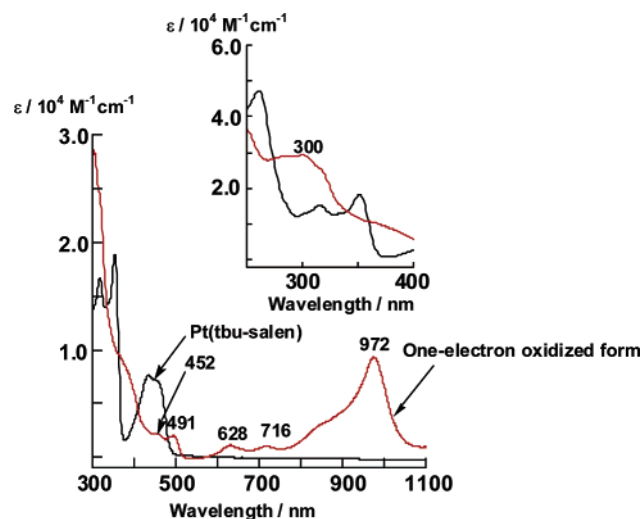
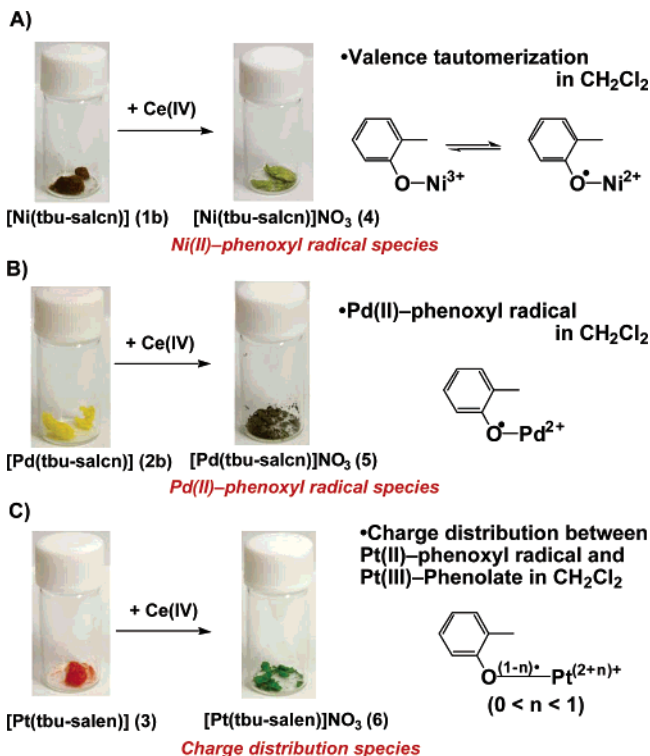


Figure 7. Absorption spectral change of **3** before and after one-electron oxidation by 1 equiv of Ce(IV) at $-40\text{ }^{\circ}\text{C}$ in CH_2Cl_2 ($5.0 \times 10^{-4}\text{ M}$): black line, **3**; red line, oxidized **3**.

most stable species among the group 10 metal–tbu-salen species. In this connection, the reaction of [Pt(salen)] with an equimolar amount of $(\text{NH}_4)_2\text{Ce}(\text{NO}_3)_6$ in CH_2Cl_2 at $-60\text{ }^{\circ}\text{C}$ caused a color change from yellow to green, though oxidation of the other group 10 metal–salen complexes resulted in immediate decomposition.^{16,28} The absorption spectrum of oxidized [Pt(salen)] exhibited a peak at λ ($\epsilon/\text{M}^{-1}\text{ cm}^{-1}$) = 385 nm (12000) and a broad peak at 708 nm (1500) but lacked the strong 972-nm band of oxidized **3**.

Although only a broad ESR signal of oxidized [Pt(salen)] was observed at around $g = 2.00$ in the range 5–240 K, oxidized **3** exhibited sharp rhombic signals and a large g tensor anisotropy ($g_1 = 2.34$, $g_2 = 1.98$, $g_3 = 1.78$, and $g_{\text{av}} = 2.03$) in the range 5–200 K (Figure 4E,F). The integrated spectrum of oxidized **3** showed that the number of the spin remained essentially the same in this temperature range, the amount of the unpaired electron being more than 0.90. The g_{av} value indicates that the unpaired electron is located mainly on the ligand, because similar g values were found for Ni(II)– and Pd(II)–phenoxy radical species (vide supra). However, the observed large g -anisotropy can arise from large orbital contributions by strong spin–orbit coupling by the Pt atom.³⁷ The rhombic ESR signals were temperature independent below $-60\text{ }^{\circ}\text{C}$. The metal orbital contribution of oxidized **3** was observed at higher temperature than those for oxidized **2a**. Oxidized **3** in CH_2Cl_2 at $-60\text{ }^{\circ}\text{C}$ exhibited a new Raman band at 1600 cm^{-1} , which is close to the 1605 and 1596 cm^{-1} bands for the Ni– and Pd–phenoxy radical complexes, respectively (Figure 6C,D). Although the ν_{7a} band around 1500 cm^{-1} is absent, this spectral feature is different from the metal-centered oxidation species such as oxidized **1** in DMF, and the result is in agreement with the observation that the Raman intensity $I(\nu_{8a})$ is higher than $I(\nu_{7a})$, as observed for metal-coordinated phenoxy radicals.^{31,32} Therefore, the 1600-cm^{-1} band may be assigned to the ν_{8a} vibration of the phenoxy radical; i.e., the unpaired electron of oxidized **3** also resides in the tbu-salen ligand. These results support that one-electron oxidation of the Pt(II) complex in CH_2Cl_2 is mainly a ligand-centered oxidation to give the Pt–

Scheme 1. Isolation of (A) [Ni(tbu-salcn)]NO₃ (**4**), (B) [Pd(tbu-salcn)]NO₃ (**5**), and (C) [Pt(tbu-salen)]NO₃ (**6**) and Their Properties



phenoxy radical species with a relatively large distribution of the Pt character.

Isolation and Characterization of Solid Radical Complexes. When solutions of one-electron-oxidized **1b**, **2b**, and **3** in $\text{CH}_2\text{Cl}_2/\text{Et}_2\text{O}$ were kept at $-80\text{ }^{\circ}\text{C}$ for a few days, the oxidized species were isolated as green powders (Scheme 1), and their formulas were determined to be [Ni(tbu-salcn)]NO₃ (**4**), [Pd(tbu-salcn)]NO₃ (**5**), and [Pt(tbu-salen)]NO₃ (**6**), respectively, by elemental analysis and ESI mass spectrometry. The absorption spectra of **4**, **5**, and **6** redissolved in CH_2Cl_2 or DMF were in good agreement with those of the one-electron-oxidized complexes before isolation. The absorption and ESR spectra and CVs demonstrated that the isolated complexes were one-electron-oxidized species.

(a) [Ni(tbu-salcn)]NO₃ (**4**). The reflectance spectrum exhibited characteristic peaks at 311, 374, 430, 881, and 1103 nm, which were similar to the absorption spectrum in CH_2Cl_2 . The CV in CH_2Cl_2 showed a reversible redox wave at $E_{1/2} = 0.81\text{ V}$, in the range 0.5–1.2 V, and the rest potential was observed at 0.85 V. The redox potential was similar to that of **1b** in CH_2Cl_2 , but the rest potential was higher. Complex **4** is therefore concluded to be one-electron-oxidized **1b**. The redox wave in DMF was observed at a lower potential ($E_{1/2} = 0.75\text{ V}$; rest potential = 0.81 V) and was much less reversible.

While a solution of **4** in CH_2Cl_2 was found to show the valence tautomerism between the Ni(III)–phenolate and Ni(II)–phenoxy radical species from the temperature dependence of the ESR spectrum, the solid-state ESR spectrum at 77 K exhibited signals at $g_1 = 2.16$, $g_2 = 2.02$, $g_3 = 2.00$, and $g_{\text{av}} = 2.06$ (Figure 8) without spectral change in the temperature range 77–300 K. This spectral feature was very different from that of one-electron-oxidized **1a** and **1b** in solution at 77 K.

(37) Möller, E.; Kirmse, R. *Inorg. Chim. Acta* **1997**, *257*, 273.

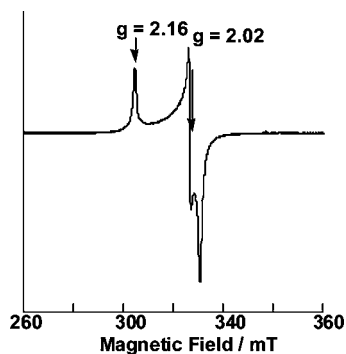


Figure 8. Solid-state ESR spectrum of **4** at 77 K. Microwave power, 1 mW; modulation amplitude, 0.63 mT.

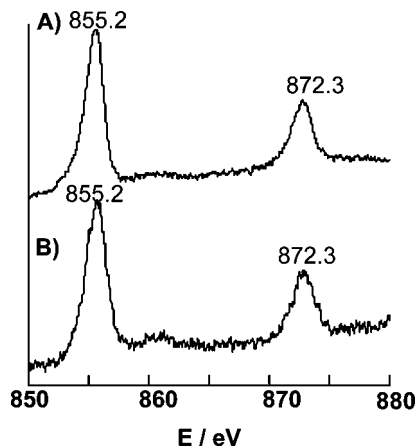


Figure 9. XPS of **1b** (A) and **4** (B).

Lovecchio et al. observed similar anisotropic spectra for the oxidized species of Ni–cyclamine complexes and assigned them to the low-spin d^7 square-planar Ni(III) complexes with $^2B_{2g}$ ground state.³⁸ On the other hand, Sellman et al. reported a similar observation on a Ni–dithiolene complex and concluded a considerable contribution of the ligand-centered SOMO.³⁹ XPS of **1b** and **4** indicated the same binding energies for Ni $2p_{1/2}$ at 872.3 eV and $2p_{3/2}$ at 855.2 eV (Figure 9). The XPS values depend on the oxidation state of the Ni ion, and the energy differences between the Ni(II) and Ni(III) states are reported to be ca. 0.8 eV for $2p_{1/2}$ and 1.0 eV for $2p_{3/2}$.⁴⁰ Since there is no difference between **1b** and **4**, the oxidation number of the Ni ion in complex **4** is determined to be +2. In addition, **1b** and **4** gave very similar XANES spectra, supporting that the oxidation states of the two metal centers are also very similar (Figure S3). Considering that the reflectance spectrum of **4** is in good agreement with the absorption spectrum of Ni–salen radical species and very different from that of the Ni(III)–salen in DMF, we conclude that the electronic structure of **4** is described by an unpaired electron occupying a phenoxyl radical-centered SOMO with a little Ni character. The observation that there is a mixing of the Ni character in the radical signals indicates that the unpaired electron is delocalized through the Ni center, and this is in agreement with the results of the recent studies.¹⁷ It should be noted in this connection that the solid

(38) Lovecchio, F. V.; Gore, E. S.; Bush, D. H. *J. Am. Chem. Soc.* **1974**, *96*, 3109.

(39) Sellman, D.; Binder, H.; Häussinger, D.; Heinemann, F. W.; Sutter, J. *Inorg. Chim. Acta* **2000**, *300–302*, 829.

(40) Colpas, J. D.; Maroney, M. J.; Bagyinka, C.; Kumar, M.; Willis, W. S.; Suib, S. L.; Baidya, N.; Mascharak, P. K. *Inorg. Chem.* **1991**, *30*, 920.

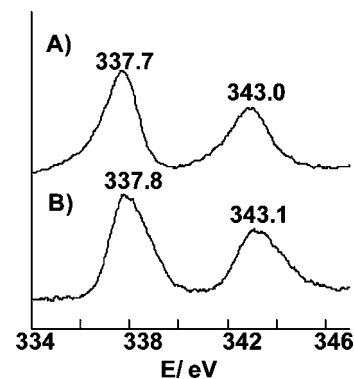


Figure 10. XPS of **2b** (A) and **5** (B).

sample of **4** did not show the valence tautomerism with the temperature. We may infer, therefore, that valence tautomerization of one-electron-oxidized Ni(II)–salen-type complexes requires dissolution in solvents. Since the Ni(II) species of salen complexes is formed only upon addition of exogenous ligands,^{16,17} formation of the Ni(III)–phenolate species in CH_2Cl_2 and $CHCl_3$ may be caused by some ligand coordination at the solvent phase transition temperature.

(b) **[Pd(tbu-salcn)]NO₃ (5)**. A solution of **5** in CH_2Cl_2 showed a reversible redox wave at $E_{1/2} = 1.04$ V, with the rest potential of 1.13 V, in the range 0.5–1.2 V, indicating that complex **5** is one-electron-oxidized **2b**. The reflectance spectrum of complex **5** exhibited peaks at 385 nm and broad peaks at 728 nm which were similar to those observed for the CH_2Cl_2 and DMF solutions of **5**. The solid-state ESR spectrum at 77 K exhibited an isotropic signal at $g = 2.01$, slightly influenced by the Pd nuclear spin. The g value is in good agreement with that of oxidized **2b** in CH_2Cl_2 , and there was no spectral change in the temperature range 77–300 K. The spectral features indicate that the unpaired electron of the one-electron-oxidized species is localized in the phenolate moiety in solution and in the solid state. Further, the XPS of complexes **2b** and **5** showed similar values of Pd $3d_{3/2}$ at 343.0 and 343.1 eV and $3d_{5/2}$ at 331.7 and 337.8 eV, respectively (Figure 10), and their XANES gave similar spectra, again indicating that the complexes have the metal center with a very similar oxidation state. The $3d_{3/2}$ and $3d_{5/2}$ XPS values are dependent on the oxidation state of the Pd ion, and a large difference between the Pd(II) and Pd(IV) complexes has been reported.⁴¹ Since the differences in the XPS values between **2b** and **5** were very small, the oxidation state of the Pd ion in complex **5** was concluded to be the +2 state.

(c) **[Pt(tbu-salen)]NO₃ (6)**. The peaks of the reflectance spectrum observed at 360, 452, 491, 628, 716, 850, and 972 nm were similar to those for a CH_2Cl_2 solution of oxidized **3**. The CV of redissolved complex **6** in CH_2Cl_2 showed a reversible redox wave at $E_{1/2} = 0.77$ V, in the range 0.5–1.2 V, with the rest potential of 0.82 V, which is higher than that for the one-electron redox process of **3**. The solid-state ESR spectrum of **6** at 77 K exhibited anisotropic signals at $g_1 = 2.34$, $g_2 = 1.98$, $g_3 = 1.78$, and $g_{av} = 2.03$, which correspond well with those of oxidized **3** in CH_2Cl_2 . There was no ESR spectral change in the temperature range 77–273 K, clearly indicating that complex

(41) Kagami, Y.; Iwahori, F.; Ohishi, T.; Hama, T.; Manabe, T.; Yamashita, M.; Kitagawa, H.; Sakai, K.; Mitani, T. *Synth. Met.* **1997**, *86*, 1803.

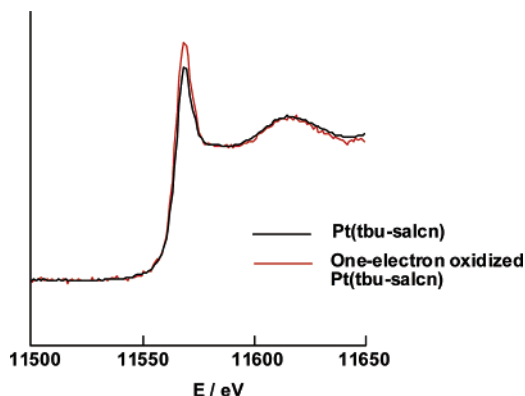


Figure 11. L_{III} -edge XANES of solid samples of **3** and **6**: black line, **3**; red line, **6**.

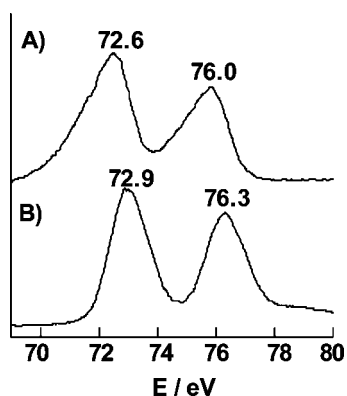


Figure 12. XPS of **3** (A) and **6** (B).

6 is one-electron-oxidized **3** and a monomeric species without a Pt–Pt bond.

The oxidation state of the Pt ion in **6** was investigated by XANES, and the normalized L_{III} XANES of **3** and **6** are shown in Figure 11. The two L_{III} absorption edges are very similar in shape, indicating that the coordination environments of the two compounds are very similar and therefore that the coordination geometry of **6** is similar to that of **3**.⁴² However, the white line intensity of **6** increased in comparison with that of **3**. In general, the density of unoccupied states was reflected in the intensity of the white line, with the energy increasing with increasing oxidation number of the metal center.⁴² Such a metal-centered oxidation feature could not be observed for the one-electron-oxidized complexes **4** and **5**; that is, the Ni and Pd complexes showed the same XANES K-edge value before and after oxidation (Figures S3 and S4). We conclude that the Pt ion in complex **6** has a higher oxidation state than in complex **3**. The XPS measurements of **3** and **6** (Figure 12) indicated that the Pt 4f binding energies of **3** are typical of the Pt(II) state, centered at 76.0 and 72.6 eV for $4f_{5/2}$ and $4f_{7/2}$, respectively, which agree well with the values of 76.1 and 72.8 eV for *cis*-[Pt^{II}Cl₂(NH₃)₂], respectively.^{43–45} On the other hand, complex **6** showed the Pt $4f_{5/2}$ and $4f_{7/2}$ binding energies of 76.3 and 72.9 eV, respectively,

which are slightly different from the corresponding values for **3** but definitely different from those of the Pt(III) or Pt(IV) complexes, e.g., 78.7 and 75.4 eV for *cis*-[Pt^{IV}Cl₄(NH₃)₂] and 77.9 and 74.6 eV for a Pt(III) complex H–H[(NO₃)Pt₂(NH₃)₄-(α -pyrrolidonato)₂(NO₂)](NO₃)₂·H₂O, assigned as the $4f_{5/2}$ and $4f_{7/2}$ binding energies, respectively.^{43–45} The small differences in the Pt $4f_{5/2}$ and $4f_{7/2}$ binding energies for **3** and **6** may suggest non-integer oxidation numbers, as reported for the tetranuclear Pt complexes containing three Pt–Pt bonds, which were determined to have the oxidation state of +2.14 to +2.5 because of the delocalization of the Pt electrons through the Pt–Pt bonds.⁴⁵ From these results, we conclude that **6** has a similar, mainly ligand-centered oxidation state with a large Pt character.

Summary and Conclusions

We prepared and characterized the salen complexes of the group 10 metal ions, Ni(II), Pd(II), and Pt(II). All the complexes have a similar structure, and their redox potentials were reversible in the narrow range of 0.8–1.1 V. We further isolated the corresponding one-electron-oxidized complexes as green solids. The electronic structures of one-electron-oxidized species depended on the central metal ion and solvents used. Thus, one-electron oxidation of [Ni^{II}(*tbu*-salen)] species in CH₂Cl₂ yielded the corresponding Ni(III)–phenolate complex at < –120 °C and the Ni(II)–phenoxy radical species at > –100 °C. The temperature-dependent conversion is regarded as a valence tautomerism governed by the solvent. The transition temperature in CHCl₃ was higher than that in CH₂Cl₂, and the tautomerism was not observed in DMF. The properties of one-electron-oxidized [Ni(*tbu*-salcn)] complex isolated as a green powder were in good agreement with those of Ni–phenoxy radical, except that the oxidation state of the green solid was independent of the temperature. One-electron-oxidized [Pd(*tbu*-salen)] was determined to be a Pd(II)–phenoxy radical species, which was the ground state with a small distribution of the radical electron spin on the Pd center in solution and in the solid state, irrespective of solvents and temperature. On the other hand, one-electron-oxidized [Pt(*tbu*-salen)] showed an oxidation state in between the Pt(III)–phenolate and Pt(II)–phenoxy radical. The charge distribution properties remained the same in the isolated green complex **6**. The solid-state ESR spectrum of **6** at 77 K was similar to that of one-electron-oxidized **3** in CH₂Cl₂, which suggests that **6** has no strong Pt–Pt bonding. These experimental results suggested that the delocalization ability of the unpaired electron in the complexes in CH₂Cl₂ is in the order **1** (valence tautomerism between Ni(II)–phenoxy and Ni(III)–phenolate) > **3** (mainly Pt(II)–phenoxy with charge distribution giving Pt(III)–phenolate) > **2** (localized Pd(II)–phenoxy radical), which is in an interesting reverse correlation with the order of the redox potential, **1** (Ni) < **3** (Pt) < **2** (Pd). Also, the order of the stability of the oxidized species in CH₂Cl₂ as viewed from the half-life of the radical, **3** (Pt) > **1** (Ni) > **2** (Pd) at –20 °C, is different from the order of the redox potential. Taken together, these observations suggest that the stability is correlated with the temperature-dependent stability of the delocalized state, and we may therefore conclude that the stability is in the observed order, i.e., **3** > **1** > **2**, at –20 °C.

The present findings demonstrate the versatile nature of the group 10 metal ions in the 2N2O-donor *tbu*-salen coordination sphere, which are similar to each other and yet characteristic of the central metal ions, and will provide further information

(42) Iwasawa, Y. *X-Ray Absorption Fine Structure for Catalysts Surfaces. Crystallography*; World Scientific Publishing Co.: London, 1995; Chapter 8.

(43) Sarnesky, J. E.; MacPhail, A. T.; Onan, K. D.; Erickson, L. E.; Relley, C. N. *J. Am. Chem. Soc.* **1977**, *99*, 7376.

(44) Barton, J. K.; Best, S. A.; Lippard, S. J.; Walton, R. A. *J. Am. Chem. Soc.* **1978**, *100*, 3785.

(45) Matsumoto, K.; Sakai, K.; Nishio, K.; Tokisue, Y.; Ito, R.; Nishide, T.; Shichi, Y. *J. Am. Chem. Soc.* **1992**, *114*, 8110.

on their functions in chemical systems. Further studies on metal–phenoxyl systems are in progress in our laboratories.

Acknowledgment. We are grateful to Prof. H. Kitagawa, Graduate School of Science, Kyushu University, and Prof. T. Kojima, Graduate School of Engineering, Osaka University, for measurement of reflectance spectra and helpful discussions. We thank Dr. M. Kobayashi, Institute for Materials Chemistry and Engineering, Kyushu University, for measurement of XPS. We also thank Ibaraki Industrial Technology Institute for measurements of XPS and solid-state resonance Raman spectra and Rigaku Corporation for measurement of XANES. The present work was supported by Grants-in-Aid for Scientific Research (No. 17750055 to Y.S. and No. 16350036 to O.Y.) from the

Ministry of Education, Culture, Sports, Science, and Technology of Japan, for which we express our sincere thanks.

Supporting Information Available: Figures showing the ^1H NMR spectra of group 10 metal complexes **1a**, **2a**, and **3** (Figure S1), the temperature dependence of the ESR spectra of oxidized **1b** in CHCl_3 (Figure S2), and K-edge XANES of solid samples of **1b** and **4** (Figure S3) and **2b** and **5** (Figure S4), and Table S1, giving crystal data for complexes **1a**, **2a**, and **3** (PDF); crystallographic data (excluding structure factors) for complexes **1**, **2**, and **3** (CIF). This material is available free of charge via the Internet at <http://pubs.acs.org>.

JA067022R